Efficient Small-Molecule Non-fullerene Electron Transporting Materials for High-performance Inverted Perovskite Solar Cells

Fei Wu,[a‡] Wei Gao,[b‡] Hui Yu,[a] Linna Zhu*[a], Lu Li*[c], Chuluo Yang*[b]

[a]*Chongqing Key Laboratory for Advanced Materials and Technologies of Clean Energy, Faculty of Materials & Energy, Southwest University, Chongqing 400715, P.R. China.*

[b]*Hubei Key Lab on Organic and Polymeric Optoelectronic Materials, Department of Chemistry, Wuhan University. Wuhan 430072, P. R. China.*

[c]*New Materials Technology Institute, Co-Innovation Center for Micro/Nano Optoelectronic Materials and Devices, Chongqing University of Arts and Sciences, Chongqing, 402160, People's Republic of China.*

***Corresponding Author**: *Linna Zhu*, *Institute for Clean Energy & Advanced Materials, Southwest University, Chongqing, China, E-mail address: lnzhu@swu.edu.cn.*

Lu Li, Chongqing University of Arts and Sciences, Chongqing, China, E-mail address: lli@cqwu.edu.cn.

Chuluo Yang, Department of Chemistry, Wuhan University. E-mail address: clyang@whu.edu.cn.

Experimental Section

Materials

In this work, all major materials were purchased from commercial suppliers and used without further purification, including P3CT (Rieke Metals), PbI_2 (*p*-OLED, >99.99 %), MAI (*p*-OLED, ≥99.5 %), PCBM (*p*-OLED, ≥99 %), C60 (*p*-OLED), BCP (*p*-OLED), Rhodamine 101 (Sigma-Aldrich), DMF (Sigma-Aldrich, 99.8 %), DMSO (Sigma-Aldrich, 99.8 %) and CB (Sigma-Aldrich, 99.8 %). ITCPTC-Se and ITCPTC-Th were synthesized according to the previous work [1].

Device Fabrication

The indium tin oxide (ITO) glass substrates were sequentially washed by sonication using detergent, deionized water, ethanol and acetone. The hole transporting layer P3CT-Na [2] was spin-coated on ITO substrates at 4000 rpm for 60 s followed by annealing at 140 °C for 30 min. Then the samples were transferred into a N_2-filled glovebox. A $CH_3NH_3PbI_3$ precursor solution (1.4 M in DMF:DMSO mixed solution with a v/v of 4:1) was spin-coated in a two-step program at 400 and 5000 rpm for 3 and 30 s, respectively. During the second step, 200 μL of chlorobenzene was poured on the spinning substrate at 10 s after the start-up. Next, the as-spun perovskite layer was annealed on a hot plate at 60 °C for 1 min and at 80 °C for 2 min to remove the solvent and form the perovskite phase. Then, PCBM, ITCPTC-Se or ITCPTC-Th solutions (15 mg/mL, 10 mg/mL, 5 mg/mL, 2 mg/mL and 1 mg/mL) in chlorobenzene were spin-coated (5000 rpm, 3000 rpm and 2000 rpm) onto the perovskite layer. To fabricate ITO/P3CT-Na/Perovskite/ETL/Rhodamine 101/LiF/Ag device, subsequently Rhodamine 101 was deposited by spin coating Rhodamine 101 solution (0.05 wt% in isopropanol) at 1000 rpm for 40 s [3]. After wards, 1 nm thick LiF was then thermally evaporated, and an approximately 100 nm thick Ag counter electrode was deposited on top to finish the device fabrication. In this device architecture, Rhodamine 101 and LiF layers work as the double interlayers between the ETL and the Ag electrode. To fabricate ITO/P3CT-Na/Perovskite/ETL/C60/BCP/Ag device, C60 (20 nm) and BCP (8 nm) were evaporated under high vacuum on top of the ETL sequentially. Finally, a 100 nm thick Ag electrode was deposited through a shadow mask. The active area of our device is 0.09 cm^2.

Characterization

UV-vis absorption spectra were measured on a Shimadzu UV-2450 absorption spectrophotometer. XRD was performed on a Japan Shimadzu XRD-7000 diffractometer. The morphology of perovskite films were characterized by FE-SEM images (JSM-7800F). AFM images were collected in air on a Bruker AFM using a tapping mode. The current–voltage (*J–V*) curves were measured under 100 mW cm^{-2} (AM 1.5 G) simulated sunlight using Keithley 2400 in conjunction with a Newport solar simulator (94043A). The external quantum efficiency (EQE) was calculated from the photocurrent measurement under monochromatic illuminations at different wavelengths, using a 150 W xenon lamp and a monochromator. Steady-state PL spectra were recorded on a Hitachi F-4600 FL Spectrophotometer. Time-resolved PL decay curves were measured by a single photon counting spectrometer from Edinburgh Instruments (FS5). The impedance spectra were measured with CHI in the dark at a bias of 0.9 V.

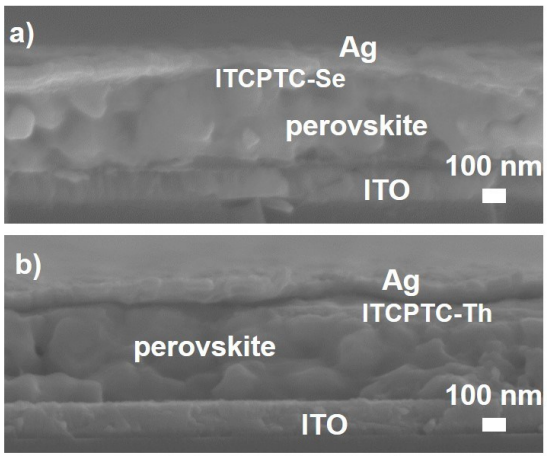

Figure S1. Cross-sectional SEM images of p-i-n perovskite solar cells with ITCPTC-based ETLs: a) ITO/P3CT-Na/Perovskite/ITCPTC-Se/Rhodamine 101/LiF/Ag, b) ITO/P3CT-Na/Perovskite/ITCPTC-Th/Rhodamine 101/LiF/Ag.

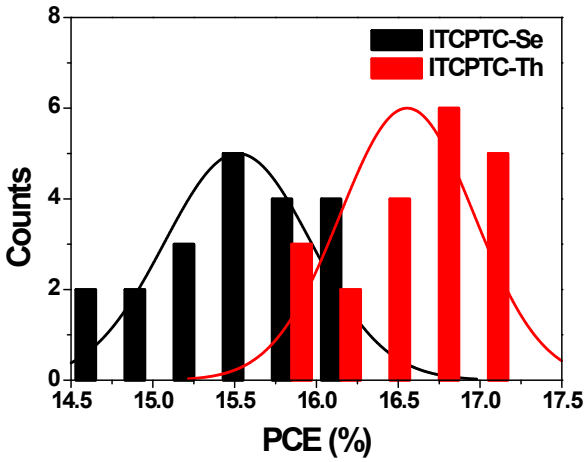

Figure S2. PCE distributions of perovskite solar cells using ITCPTC-based ETLs.

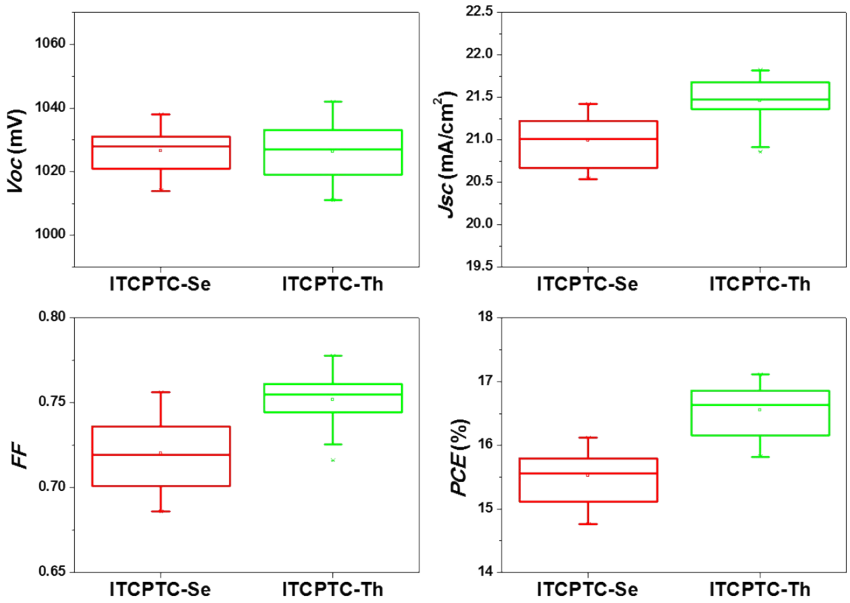

Figure S3. Photovoltaics parameters statistic for ITCPTC-Se or ITCPTC-Th as ETL (ITO/P3CT-Na/Perovskite/ITCPTC-(Se or Th)/Rhodamine 101/LiF/Ag).

Table S1. Forward and reverse scan of PSCs using ITCPTC-Se or ITCPTC-Th as ETLs.

Device	V_{oc} (mV)	J_{sc} (mA cm^2)	*FF*	PCE (%)
ITCPTC-Se (forward)	1030	21.24	0.74	16.12
ITCPTC-Se (reverse)	1033	21.24	0.72	15.84

ITCPTC-Th (forward)	1029	21.77	0.76	17.11
ITCPTC-Th (reverse)	1034	21.76	0.76	17.10

Table S2. Summary of the photovoltaic performances of PSCs with ITCPTC-Se ETL in different thicknesses.

ITCPTC-Se	V_{oc} (mV)	J_{sc} (mA cm^2)	*FF*	PCE (%)
8 nm	538	17.40	0.46	4.28
23 nm	993	19.63	0.68	13.37
29 nm	1028	20.56	0.69	14.67
34 nm	1030	21.24	0.74	16.12
43 nm	1035	20.01	0.70	14.59

Table S3. Summary of the photovoltaic performances of PSCs with ITCPTC-Th ETL in different thicknesses.

ITCPTC-Th	V_{oc} (mV)	J_{sc} (mA cm^2)	*FF*	PCE (%)
5 nm	420	16.64	0.40	2.82
10 nm	949	19.46	0.56	10.30
31 nm	1032	20.34	0.71	14.95
35 nm	1019	21.46	0.75	16.41
42 nm	1029	21.77	0.76	17.11
48 nm	991	20.75	0.73	15.09

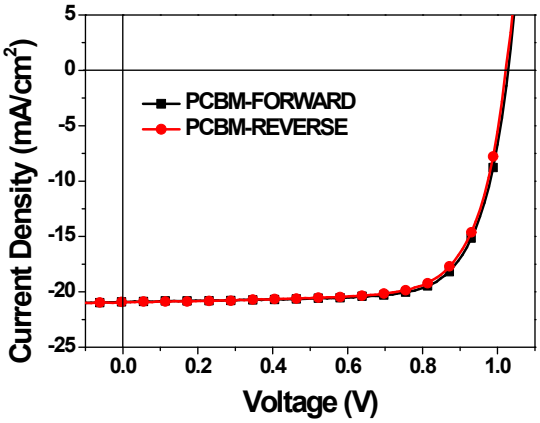

Figure S4. *J-V* curves of PSCs using PCBM as ETL. Device structure: ITO/P3CT-Na/Perovskite/PCBM/Rhodamine 101/LiF/Ag.

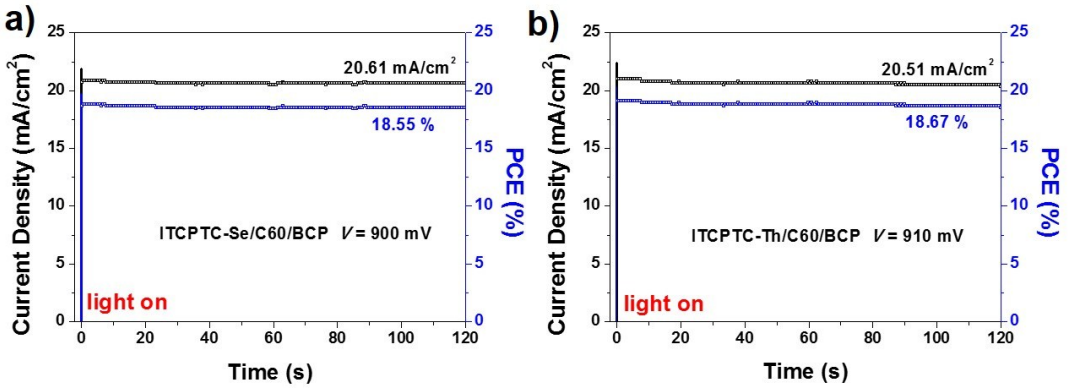

Figure S5. Stabilized photocurrent density and efficiency output of a) ITCPTC-Se-based device; b) ITCPTC-Th-based device. In these devices, ITCPTC-compounds work as the interlayer.

Table S4. Forward and reverse scan of PSCs using ITCPTC-Se or ITCPTC-Th as interlayer. Control refers to devices using C_{60}/BCP without the interlayer.

	V_{oc} (mV)	J_{sc} (mA cm^{-2})	*FF*	PCE (%)
ITCPTC-Se/C_{60}/BCP (Forward)	1053	22.32	0.79	18.62
ITCPTC-Se/C_{60}/BCP	1033	22.27	0.79	18.54

(Reverse)				
ITCPTC-Th/C_{60}/BCP	1029	22.54	0.78	18.75
(Forward)				
ITCPTC-Se/C_{60}/BCP	1034	22.47	0.78	18.69
(Reverse)				
Control (Forward)	1038	21.51	0.77	17.10
Control (Reverse)	1038	21.41	0.76	16.93

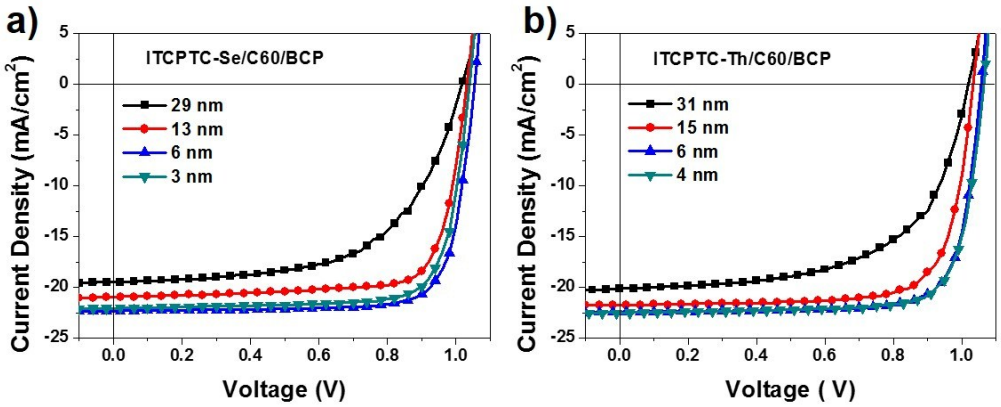

Figure S6. *J-V* curves of PSCs with ITCPTC-Se or Th **interlayer** in different thicknesses.

Table S5. Summary of the photovoltaic performances of PSCs with ITCPTC-Se **interlayer** in different thicknesses.

ITCPTC-Se	V_{oc} (mV)	J_{sc} (mA cm^{-2})	*FF*	PCE (%)
29 nm	1017	19.51	0.59	11.79
13 nm	1032	20.94	0.77	16.68
6 nm	1053	22.32	0.79	18.62
3 nm	1039	22.07	0.78	17.92

Table S6. Summary of the photovoltaic performances of PSCs with ITCPTC-Th **interlayer** in different thicknesses.

ITCPTC-Th	V_{oc} (mV)	J_{sc} (mA cm^{-2})	*FF*	PCE (%)
31 nm	1020	20.15	0.60	12.29
15 nm	1035	21.78	0.76	17.02
6 nm	1055	22.45	0.79	18.75
4 nm	1064	22.54	0.78	18.75

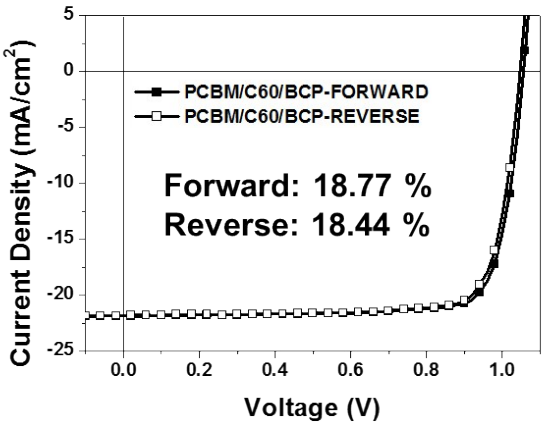

Figure S7. Forward and reverse scan of inverted PSCs based on PCBM interlayer.

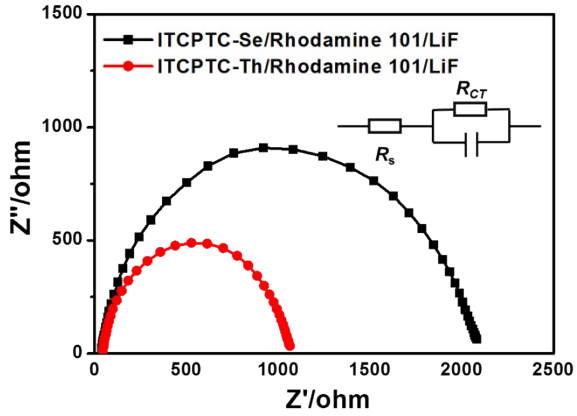

Figure S8. Nyquist plots of PSCs with ITCPTC-Se/Th ETLs measured in the dark condition. Inset is the equivalent circuit model.

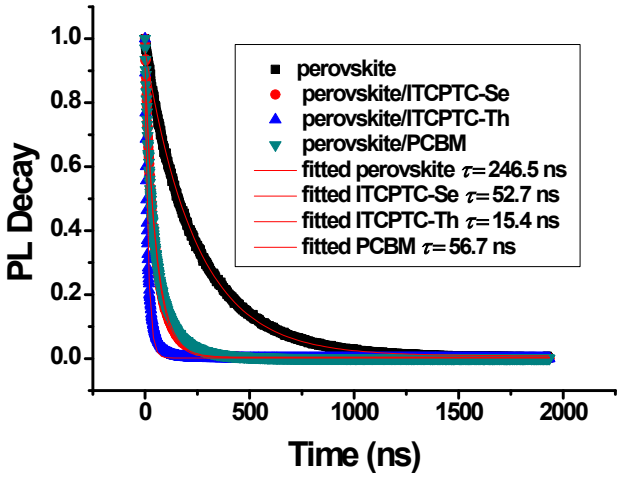

Figure S9. Fitted PL decays of perovskite, perovskite/ITCPTC-Se and perovskite/ITCPTC-Th, respectively.

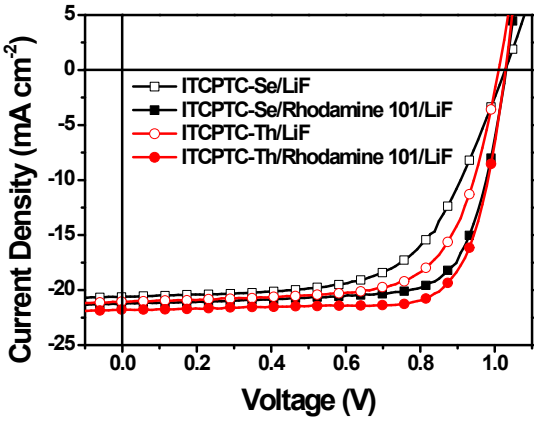

Figure S10. *J-V* curves of inverted PSCs with and without the Rhodamine 101 buffer layer. The device structure is: ITO/P3CT-Na/Perovskite/ETL/**with or without** Rhodamine 101/LiF/Ag.

Table S7. Summary of the photovoltaic performances of PSCs with and without the Rhodamine 101 buffer layer.

Device	V_{oc} (mV)	J_{sc} (mA cm^2)	*FF*	PCE (%)
ITCPTC-Se/LiF	1028	20.63	0.62	13.08
ITCPTC-Se/Rhodamine 101/LiF	1030	21.24	0.74	16.12

ITCPTC-Th/LiF	1011	21.05	0.69	14.71
ITCPTC-Th/Rhodamine 101/LiF	1029	21.77	0.76	17.11

References:

[1] W. Gao, Q. An, R. Ming, D. Xie, K. Wu, Z. Luo, Y. Zou, F. Zhang, C. Yang, Adv. Funct. Mater. 27 (2017) 1702194.

[2] X. Li, X. Liu, X. Wang, L. Zhao, T. Jiu, J. Fang, J. Mater. Chem. A 3 (2015) 15024-15029.

[3] K. Sun, J. Chang, F. H. Isikgor, P. Li, J. Ouyang, Nanoscale 7 (2015) 896-900.